2018 IEEE Intelligent Vehicles Symposium (IV)
Changshu, Suzhou, China, June 26-30, 2018

Adaptive Anti-slip Regulation Method for Electric Vehicle with In-wheel Motors Considering the Road Slope

Bin Li, Lu Xiong and Bo Leng

***Abstract*—Anti-slip regulation (ASR) is one of the research focus in the field of active safety of electric vehicle. An ASR algorithm adaptive to road condition is proposed in this paper based on 4WD electric vehicle with in-wheel motors. The controller based on anti-windup sliding mode control is robust to wheel parameter uncertainty. The longitudinal velocity estimator based on the fusion of dynamics method and kinematics method is adopted to reduce the velocity estimation error. The road slope is estimated using recursive least square with forgetting factor and the longitudinal acceleration sensor information is calibrated by the road slope estimation for slope adaptive velocity estimation. At the same time, a road coefficient estimator is adopted to estimate road condition using improved Burckhardt model, so the optimal reference slip ratio is selected according to the estimated road adhesion coefficient for the maximum driving efficiency and the realization of adaptive anti-slip regulation. Multi-condition simulations show that the controller is adaptive to road changes, and it can suppress wheel slip ratio and ensure the vehicle stability.**

I. INTRODUCTION

Anti-slip regulation (ASR) is of great importance in improving vehicle's driving performance, stability and safety. The researches on slip ratio control of electric vehicle with in-wheel motors have gained increasing attention lately. Hori [1] proposed an ASR algorithm using model following control (MFC), and only the torque and motor speed are required, but the strategy can only control the slip ratio to zero, hence the loss of driving efficiency. Subudhi [2] devised a sliding mode controller (SMC) adaptive to different road conditions, but the motor torque chatters a lot.

The accurate knowledge of the maximum road adhesion coefficient and vehicle velocity is important for ASR. Gustafsson [3] used the slope of $\mu-\lambda$ curve in small λ area to estimate the peak road adhesion coefficient, but it cannot provide acceptable estimation on extreme working conditions. In [4], nonlinear tire models are used to fit the $\mu-\lambda$ curve in high λ area and the μ where the derivative of the curve is zero is considered as the peak road adhesion coefficient. But this method depends on highly accurate tire models. As for the velocity estimation, the kinematics and dynamics methods both have the merits and drawbacks. Also the fusion of kinematics and dynamics method is adopted in [5] and [6], which enhances the robustness against sensor bias and model errors. However, the gravity information is included in the output of the accelerometer, thus the road slope is necessary to be recognized. Similarly, the methods of slope estimation are mainly kinematics and dynamics methods. GPS is often used in kinematic estimation method but the refresh rate is low [7]. And in [8], an algorithm using adaptive extended Kalman filter is proposed to estimate the road slope based on the vehicle longitudinal dynamics.

An integrated dynamics-kinematics vehicle velocity estimator is devised in this paper and the road slope is also estimated to correct the output information of acceleration sensor. The improved Burckhardt tire model is used to estimate the longitudinal tire force and peak road adhesion coefficient for the realization of the adaptive anti-slip regulation. In this paper, an anti-windup sliding mode controller with anti-saturation integral part is employed. In addition to the robustness of SMC, the introduction of integral part eliminates the steady-state error, and the algorithm replaces the sign function with saturation function to reduce chattering in motor torque.

II. SYSTEM STRUCTURE

The structure of the control algorithm this paper proposed is shown in Fig. 1.The controller consists of three components including the velocity estimator, the road estimator and the wheel speed controller. The velocity estimator is composed of a kinematics and a dynamics estimator and a switcher among them. Also the road slope estimator is a fusion of kinematics-dynamics estimator. The road estimator consists of two estimators including the longitudinal force estimator and the peak road adhesion coefficient estimator, the two estimators disturb with each other and have global asymptotic Lyapunov stability [9]. In the end, the wheel speed controller also has two parts, one part searches for the optimum slip ratio and calculates the corresponding reference wheel speed according to the result from the road estimator. The other

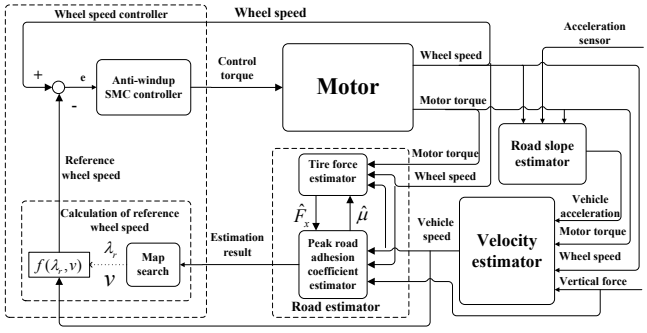

Figure 1. Controller structure.

*Resrach supported by 'National key Research and Development Program of China' (Grant No. 2016YFB0100901) and 'National Natural Science Foundation of China' (Grant No. 51475333).

Bin Li, Lu Xiong, Bo Leng are with the School of Automotive Studies, Tongji University, Shanghai, 201804, China (corresponding author: Lu Xiong; e-mail: xiong_lu@tongji.edu.cn).

controls the actual wheel speed converging to the reference value, and the algorithm is based on an anti-windup SMC controller.

III. VELOCITY ESTIMATOR

The basic wheel dynamics of electric vehicle with in-wheel motors can be illustrated by the simple 2-DOF single wheel model as shown in Fig. 2.

The dynamics of the wheel model can be described as

$$\begin{aligned} J\dot{\omega} &= T - rF_x \\ F_x &= F_z\mu(\lambda) \end{aligned} \tag{1}$$

Where F_x is the longitudinal force; F_z is the vertical force; ω is the wheel angular speed; J is the moment of inertia of the wheel; T is the torque delivered to the wheel from the actuator; r is the rolling radius of tire; μ is the nonlinear relationship between wheel slip λ and normalized longitudinal force.

And the wheel slip ratio in driving condition is defined as

$$\lambda = \frac{\omega r - v}{\omega r} \tag{2}$$

Where v is vehicle longitudinal velocity.

A. Dynamics Estimator in Low Slip Ratio Condition

The tire model is linear when the wheel slip ratio is low, so the dynamics-based method of velocity estimation can achieve fairly precision when the tire model is easy to fit in low slip ratio region. And according to the definition of slip ratio in (2), the dynamic of slip ratio is obtained in (3).

$$\dot{\lambda} = (1-\lambda)\frac{T - rF_z\mu(\lambda)}{J\omega} - \frac{\dot{v}}{\omega r} \tag{3}$$

So the corresponding dynamics estimator is (4).

$$\dot{\hat{\lambda}} = (1-\hat{\lambda})\frac{T - r\hat{F}_z\hat{\mu}(\hat{\lambda})}{J\omega} - \frac{\dot{\hat{v}}}{\omega r} \tag{4}$$

Where $\hat{\lambda}$, $\hat{v}$, $\hat{\mu}$ and $\hat{F}_z$ are the estimations of λ, v, μ and F_z respectively.

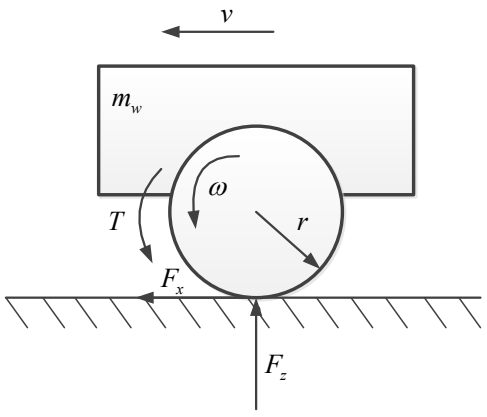

Figure 2. 2-DOF single wheel model.

The differential of the estimation error is shown in (5).

$$\dot{\tilde{\lambda}} = (1-\hat{\lambda})\frac{r(F_z\mu(\lambda) - \hat{F}_z\hat{\mu}(\hat{\lambda}))}{J\omega} - \frac{\tilde{a}_x}{\omega r} + \frac{rF_z\mu(\lambda) - T}{J\omega}\tilde{\lambda} \tag{5}$$

Where $\tilde{\lambda}$ is the error between the estimation and the actual value; $\tilde{a}_x$ is the measurement error of longitudinal vehicle acceleration. Finally the error of the estimator can be expressed as (6). Where C is the slope at the origin of the $\mu - \lambda$ curve; t_0 and t is the beginning and the end time of the estimator respectively.

$$\begin{aligned} \left\|\tilde{\lambda}\right\| \le \left\|\tilde{\lambda}(t_0)\right\| \exp[-\frac{rCF_z}{J\omega_{\max}}(t-t_0)] + \\ \sup_{t_0\le\tau\le t}(\frac{\left\|\tilde{F}_z\right\|}{F_z}\frac{\mu(\hat{\lambda})}{C} + \frac{\hat{F}_z}{F_z}\frac{\left\|\tilde{\mu}(\hat{\lambda})\right\|}{C} + \frac{J\left\|\tilde{a}_x\right\|}{(1-\hat{\lambda})r^2CF_z}) \end{aligned} \tag{6}$$

It is obvious that exponential function can rapidly reach convergence since F_z is large. The rest represent respectively the error of the vertical force estimation, tire model and acceleration measurements. The first one has little influence on the error. The last one can be ignored as the denominator is large enough, so the estimator performance is mainly dependent on accuracy of the tire model.

B. Kinematics Estimator in High Slip Ratio Condition

When the wheel skids badly, the tire model is nonlinear and difficult to build accurately, so the slip ratio estimator is modeled based on the kinematics equation. The duration of kinematics method should be limited to avoid the accumulation of signal error including the acceleration and wheel speed. And the wheel speed controller adopted can ensure that the high slip ratio duration is short enough so that the kinematics estimator can exit at suitable time.

The dynamic of slip ratio is obtained as follows:

$$\dot{\lambda} = (1-\lambda)\frac{\dot{\omega}}{\omega} - \frac{\dot{v}}{\omega r} \tag{7}$$

The corresponding kinematics estimator is (8).

$$\dot{\hat{\lambda}} = (1-\hat{\lambda})\frac{\dot{\hat{\omega}}}{\omega} - \frac{\dot{\hat{v}}}{\omega r} \tag{8}$$

The derivative of the wheel angular speed $\dot{\omega}$ can be easily influenced by the noise, so the angular acceleration of the wheels $\dot{\hat{\omega}}$ is calculated based on FIR filter using the instant wheel speed signal and the former five wheel speed signal [10]. And the equation is (9).

$$\dot{\omega} = \sum_{i=0}^{N-1}\frac{6}{N(N+1)}\cdot(1-\frac{2i}{N-1})\cdot\omega_{i+1} \tag{9}$$

Where N is the number of the sampling signals used to calculate the angular acceleration; ω_i is the wheel speed signal in chronological order.

The differential of the estimation error is shown in (10).

$$\dot{\tilde{\lambda}} = -\frac{\dot{\hat{\omega}}}{\omega}\tilde{\lambda} + (1-\lambda)\frac{\tilde{\dot{\omega}}}{\omega} - \frac{\tilde{a}_x}{\omega r} \tag{10}$$

Finally the error of the estimator can be expressed as (11).

$$\left\|\tilde{\lambda}\right\| \le \left\|\tilde{\lambda}(t_0)\right\| \exp[-\frac{\hat{\dot{\omega}}}{\omega_{\max}}(t-t_0)] + \sup_{t_0 \le \tau \le t} \frac{1}{\hat{\omega}}[(1-\lambda)\left\|\tilde{\dot{\omega}}\right\| + \frac{\left\|\tilde{a}_x\right\|}{r}] \tag{11}$$

When the wheel skids rapidly, $\hat{\dot{\omega}} / \omega$ is large without the slip ratio controller so the exponential function of base e can reach convergence timely. However, the time of large $\hat{\dot{\omega}}$ is not very long if the controller is applied. Hence appropriate switcher is required to make sure that it can restrain error accumulation.

The integrated estimator with switcher is as follows: When the difference of wheel speed $\Delta\omega$ in a sampling period is detected beyond the threshold $\omega_{threshold}$, the preparatory velocity v_{acc} is estimated based on the integration of acceleration, and the flag of wheel speed $flag\_\omega$ turns to 1, which means the wheel may be slipping.

Then only when the wheel angular acceleration exceeds the threshold $\dot{\omega}_{threshold}$ after the flag of wheel angular speed becomes 1 can it proves the skid of the wheel. This dual-flag is designed to avoid the misjudgment caused by the noise of wheel angular speed measurement. After that, the estimated preparatory velocity is used to calculate the slip ratio as the output of the estimator and it switches to kinematics estimator if the two flags both remain 1 for a period of Δt .

After the kinematics estimator holds for a period of ΔT , it is supposed that the wheel slip ratio becomes low as a result of wheel speed controller, then it turns to the dynamics estimator.

C. Velocity Estimator Based on Slip Ratio Estimation

The velocity estimator is designed with feedback from wheel speed as shown in (12).

$$\dot{\hat{v}} = sat\left(\hat{a}_x - L\left(\frac{\hat{v}}{(1-\hat{\lambda})r} - \omega\right)\right) \tag{12}$$

The differential of estimation error is obtained as (13).

$$\dot{\tilde{v}} = \dot{\hat{v}} - \dot{v} = \tilde{a}_x - \frac{L}{r}\left(\frac{\tilde{v}}{1-\hat{\lambda}} + \frac{v\tilde{\lambda}}{(1-\hat{\lambda})(1-\lambda)}\right) \tag{13}$$

Finally the error of the estimator can be expressed as (14).

$$\left\|\tilde{v}\right\| \le \left\|\tilde{v}_0\right\| \exp[-\frac{L}{r(1-\hat{\lambda})}(t-t_0)] + \sup_{t_0 \le \tau \le t}[\frac{v}{1-\lambda}\left\|\tilde{\lambda}\right\| + \frac{r}{L}(1-\hat{\lambda})\left\|\tilde{a}_x\right\|] \tag{14}$$

So the suitable L can increase the error convergence rate.

A four-wheel velocity estimation fusion strategy is proposed: the weighting coefficient of each of the four estimations should increase with the ratio of road adhesion coefficient and slip ratio estimation. And the weighting coefficient of estimation from dynamics estimator should be greater than that of kinematics estimator.

IV. Road Slope Estimation

The fusion of dynamics method and kinematics method [11] of the road slope estimation is shown as follows:

A. Dynamics Method

The dynamics method is based on the longitudinal dynamic model of the vehicle:

$$F_x = m\dot{v}_x + \frac{1}{2}\rho C_d A v_x^2 + mg(\sin\alpha + f\cos\alpha) \tag{15}$$

Where m is the vehicle mass, which is assumed to be known whether by measurement or estimation; $\dot{v}_x$ is vehicle longitudinal acceleration; ρ is the air density; C_d is the drag coefficient; A is the windward area; v_x is the vehicle longitudinal velocity; g is gravitational acceleration; α is the road slope; f is the rolling resistance coefficient.

The equation (15) is simplified to $\varphi = u + b$ after we define $\varphi = F_x$, $u = m\dot{v}_x + 0.5\rho C_d A v_x^2$, $b = mg(\sin\alpha + f\cos\alpha)$. The longitudinal driving force can be obtained from motor torque. The wheel speed $r\omega$ is used to replace the vehicle longitudinal velocity as it is supposed that the wheel slip ratio is low as a result of the wheel speed controller, so u is known. Then b can be obtained using the recursive least square (RLS) with forgetting factor [12] in consideration of the time-varying road slope.

Therefore the estimation of the road slope is:

$$\alpha_d = \arcsin\frac{b - f\sqrt{m^2g^2(1+f^2) - b^2}}{(1+f^2)mg} \tag{16}$$

B. Kinematics Method

The measurement of acceleration sensor is determined both by the vehicle acceleration and the road slope as shown in (17).

$$a_{sensor,x} = \dot{v}_x + g\sin\alpha_k \tag{17}$$

Then the road slope estimation based on the kinematic method is obtained as follows:

$$\alpha_k = \arcsin(\frac{a_{sensor,x} - \dot{v}_x}{g}) \tag{18}$$

C. Integrated Estimation Method

Considering that most measurement noise of the sensor is low frequency while the noise of dynamics method based on model parameters is high frequency mostly, filter is used to extract the useful information from the two estimations in (19).

$$\alpha = \frac{Ts}{Ts+1}\alpha_k + \frac{1}{Ts+1}\alpha_d \tag{19}$$

Where T is the positive constant to be designed.

V. Road Estimator

Compared with the widely-used Burckhardt tire model, the parameters of the Burckhardt tire model in [13] are increased from three to five parameters. The modified

Burckhardt tire model is able to describe the real tire longitudinal characteristic more accurately. The modified Burckhardt tire model is shown as follows:

$$\mu(\lambda,\theta)=\theta_1-\theta_1\exp[-\frac{\theta_2}{\theta_1}(\lambda+\theta_5\lambda^2)]-\theta_3\lambda\,\mathrm{sgn}(\lambda)+\theta_4\lambda^2 \quad (20)$$

Where θ_1 is the peak road adhesion coefficient, which is referred to as θ in later text; θ_2 is the longitudinal stiffness, which is the slope of $\mu-\lambda$ curve at origin; $\theta_3\sim\theta_5$ are parameters used to describe $\mu-\lambda$ curve in large slip ratio region and they change a little under different road conditions. In addition, θ_2 has little influence on the peak value of the curve. Then the tire model curve is only determined by peak road adhesion coefficient θ as $\theta_2\sim\theta_5$ can be set to constant [14].

Inspired by the method of Grip in [9], equation (21) is used to estimate the peak road adhesion coefficient.

$$\begin{aligned}\dot{y}&=-\frac{K_i}{J}(T+r\hat{F}_x)+\frac{rF_z}{J}f(t,\omega,\hat{\phi},\hat{\theta})\cdot\frac{\partial\mu(t,\omega,\hat{\theta})}{\partial\hat{\theta}}\\ \hat{F}_x&=\frac{J}{r}(y+K_i\omega)-F_z\cdot\mu(t,\omega,\hat{\theta})\\ \dot{\hat{\theta}}&=\gamma[\theta^*(t,\omega,\hat{F}_x)-\hat{\theta}]:=f(t,\omega,\hat{\phi},\hat{\theta})\end{aligned} \quad (21)$$

Where K_i and γ are observer parameters; θ^* is the numerical solution of function $F_x(t,\omega,\theta)=\hat{F}_x$.

The algorithm proposed in this paper adjusts the optimal reference slip ratio based on the estimation of peak road adhesion coefficient. Then the adaptive control under different road conditions is realized. The optimal reference is obtained by making the differential of the tire model (20) equal to zero.

VI. Wheel Speed Controller

According to the definition of slip ratio, it can be seen that the optimal slip ratio is equivalent to the optimal wheel angular speed as shown in (22). Where λ_r is optimal slip ratio and ω_r is corresponding optimal wheel angular speed. And $v_{\min}$ is a preset minimum speed adopted to prevent impact to reference value at low speed caused by vehicle speed error. Considering that the slip ratio is sensitive to vehicle speed estimation when the vehicle is at low speed, the slip ratio controller is designed to track the optimal wheel angular speed. The online peak road adhesion coefficient estimator sends the result to the wheel speed controller, the controller searches for the corresponding optimum slip ratio to calculate the reference wheel speed.

$$\omega_r=\frac{\max(v,v_{\min})}{r(1-\lambda_r)} \quad (22)$$

Define the tracking error $e=\omega-\omega_r$, then combining the wheel dynamics in (1) the dynamic of e is shown as

$$J\dot{e}=\varphi(e,t)+b(\lambda_r,t)+T-\bar{T}/2 \quad (23)$$

Where $\bar{T}$ is the motor torque upper limit and

$$\begin{aligned}\varphi(e,t)&=rF_z\left(-\mu(\hat{\theta},\omega_r,e)+\mu(\hat{\theta},\omega_r)\right)\\ b(\lambda_r,t)&=-rF_z\mu(\hat{\theta},\omega_r)+\bar{T}/2\end{aligned} \quad (24)$$

Inspired by the conditional integrator in [15], an anti-windup SMC controller is adopted to prevent the integral part from being too large to deteriorate the dynamic response of the system by suppressing overshoot and to restrain the chattering by employing continuous boundary layer near the sliding face. The control algorithm is shown in (25).

$$\begin{aligned}\dot{\rho}&=-k_0\rho+\delta sat\left(\frac{e+k_0\rho}{\delta}\right),|\rho(0)|\le\frac{\delta}{k_0}\\ T&=-\frac{1}{2}\bar{T}sat\left(\frac{e+k_0\rho}{\delta}\right)+\frac{1}{2}\bar{T}\end{aligned} \quad (25)$$

Where ρ is the intermediate state variable, and $\dot{\rho}=e$; k_0 and δ are positive constants to be designed.

VII. Simulation Results

The simulation platform used in this paper is a distributed drive electric vehicle with four in-wheel motors. Parameters of the vehicle and motor are shown in Table I and Table II. And the simulations are carried out in the CarSim and MATLAB/Simulink environment.

A. Correction of acceleration with slope estimation

The simulation test is on the road with a slope of 6 degrees. From the result in Fig. 3(a)-(b), it can be seen that the road slope estimation is close to the actual value and the velocity estimation with acceleration correction is more accurate than the one without acceleration correction to the output information of the acceleration sensor. “wco” , “actu” and “woco” in the legends are short for “estimation with acceleration correction ” , “actual velocity” and “estimation without acceleration correction ”respectively.

TABLE I. Parameters of the vehicle

Parameter	Value	Parameter	Value
Vehicle mass (kg)	2455	Yaw moment of inertia (kg·m²)	4557
Wheel base(m)	2.74	Distance from front axle to mass center(m)	1.227
Tire rolling radius(m)	0.35	Reduction ratio	6.2
Front track(m)	1.89	Rear track(m)	1.80

TABLE II. Parameters of the motor

Parameter	Value	Parameter	Value
Maximum torque(Nm)	250	Rated torque(Nm)	125
Maximum power(kW)	97	Rated power(kW)	40
Maximum speed(rpm)	10000	Rated speed(rpm)	3700

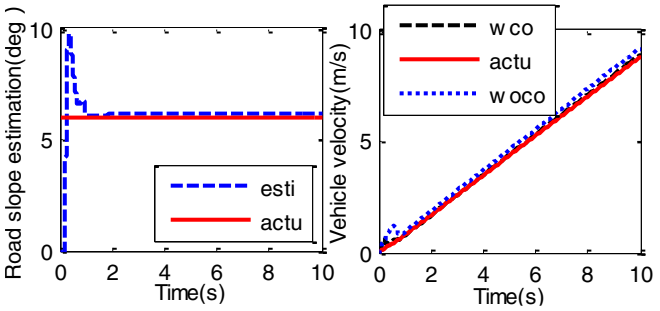

(a). Road slope estimation (b). Vehicle velocity estimation

Figure 3. Compare of velocity estimation

B. *Low μ road condition*

The simulation test condition is set as follows: the vehicle starts on a road with a slope of 6 degrees with full throttle at 0.1km/h, and the peak road adhesion coefficient is 0.2. The velocity estimation is used in the wheel speed controller. In order to simulate the real working condition, white noise with 0.2 rad/s amplitude is added into wheel angular speed signal, white noise with 0.2 m/s^2 amplitude is added into longitudinal acceleration signal and 0.005s time delay is added into the output of the motor. The simulation results of the left front wheel are shown in Fig. 4(a)-(f). "esti" and "actu" in the legends are short for "estimated" and "actual" respectively.

The results show that velocity estimation is close to the actual vehicle speed and the final velocity estimation error is less than 3%. And the slip ratio can follow the optimum value efficiently.

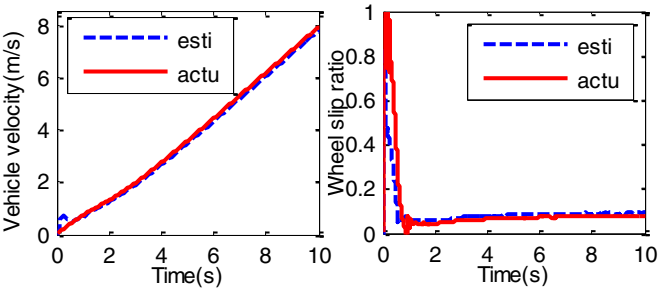

(a). Vehicle velocity estimation (b). Wheel slip ratio

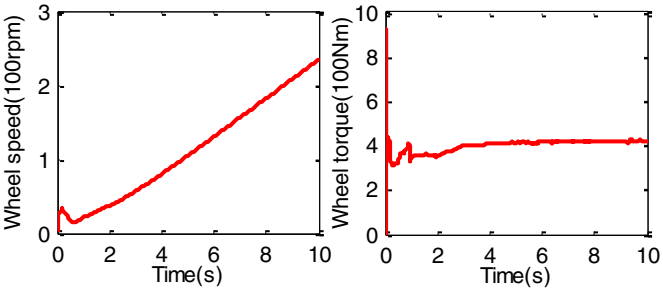

(c). Wheel speed (d). Wheel torque

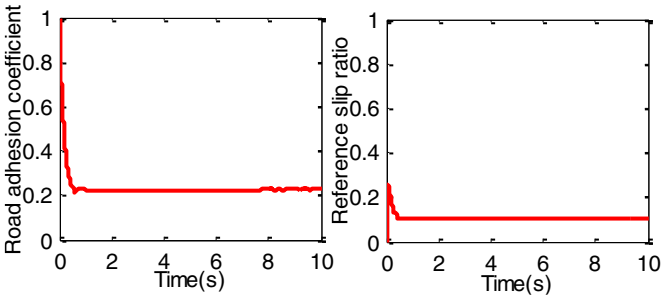

(e). Road estimation (f). Reference slip ratio

Figure 4. Simulation results of low u road condition

From the result of road estimator, it is clear that the estimator can identify the peak road adhesion coefficient in less than 1s. From the wheel torque and the slip ratio diagram, it is clear that the algorithm prevents the wheel speed from surging and increases the usage of the motor torque.

C. *Joint road condition*

The simulation test condition is set as follows: the vehicle starts with full throttle at 0.1km/h. The road slope is 6 degrees, and the peak road adhesion coefficient is set to 0.6 for the first 4 seconds, then it changes to 0.2. The perturbation and noise in the simulation is the same as that of the low μ road condition. Simulation results of the left front wheel are shown in Fig. 5(a)-(f).

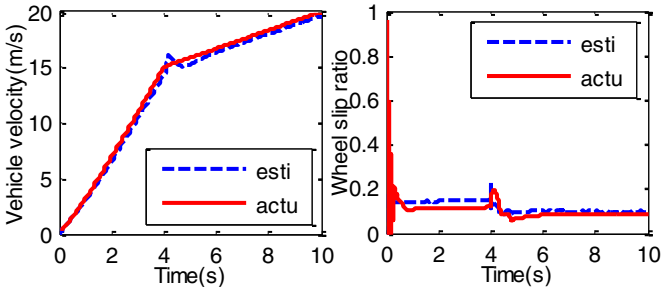

(a). Vehicle velocity estimation (b). Wheel slip ratio

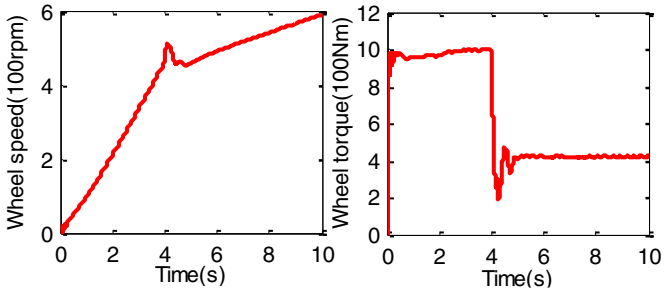

(c). Wheel speed (d). Wheel torque

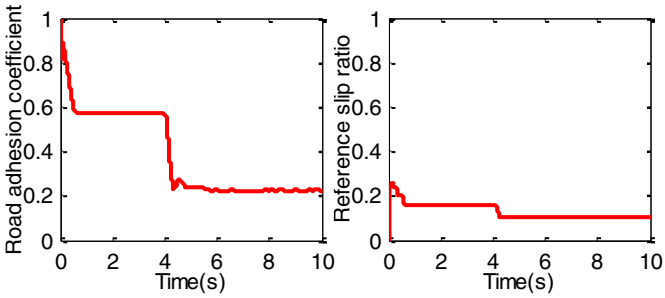

(e). Road estimation (f). Reference slip ratio

Figure 5. Simulation results of joint road condition

It can be seen from the results that the control algorithm can reduce the wheel slip ratio to the reference in less than 1s after the road changes to improve the vehicle stability. And the torque decreases to the appropriate lever after the change of the peak road adhesion coefficient. And the road estimator can detect the road change quickly as shown in (e). At the same time the velocity estimation is close to the actual value.

VIII. CONCLUSION

The main contribution of this paper is that a road adaptive slip ratio control algorithm considering the road slope is proposed for electric vehicles with in-wheel motors. The vehicle velocity is obtained using the integrated dynamics-kinematics method. Similarly, the road slope estimator based on the fusion of dynamics and kinematics method can recognize the road slope to calibrate the acceleration sensor information. The road estimator is adopted to ensure that the control algorithm is robust to the change of road conditions. And the slip ratio controller is an anti-windup SMC controller where the wheel speed is taken as control variable to avoid disturbance of slip ratio at low speed. Simulations show that the result of the vehicle velocity estimator and road slope estimator is close to the actual value. The final velocity estimation error is less than 3%. The road estimator can obtain the actual peak road adhesion coefficient in 1s. The algorithm can control the slip ratio converging to the reference slip ratio in less than 1s on low tire-road friction road and joint road.

REFERENCES

[1] Hori, Yoichi. "Future vehicle driven by electricity and control-research on four wheel motored UOT Electric March II." IEEE Transactions on Industrial Electronics 51.5, pp. 954-962, 2004.

[2] Subudhi, Bidyadhar, and S. S. Ge. "Sliding-Mode-Observer-Based Adaptive Slip Ratio Control for Electric and Hybrid Vehicles." IEEE Transactions on Intelligent Transportation Systems 13.4, pp. 1617-1626, 2012.

[3] Lee, Chankyu, K. Hedrick, and K. Yi. "Real-time slip-based estimation of maximum tire-road friction coefficient." IEEE/ASME Transactions on Mechatronics 9.2, pp. 454-458, 2004.

[4] Muller, Steffen. "Estimation of the Maximum Tire-Road Friction Coefficient." Epilepsy Research 108.2, pp. 327-330, 2003.

[5] Nishio, Akitaka, et al. "Development of Vehicle Stability Control System Based on Vehicle Sideslip Angle Estimation." SAE 2001 World Congress, 2001.

[6] Piyabongkarn, Damrongrit, et al. "Development and Experimental Evaluation of a Slip Angle Estimator for Vehicle Stability Control." IEEE Transactions on Control Systems Technology 17.1, pp. 78-88,2009.

[7] Bae, H. S., J. Ryu, and C. Gerdes. "Road grade and vehicle parameter estimation for longitudinal control using GPS." IEEE Intelligent Transportation Systems Proceedings, 2001.

[8] Liao, Xiaoyong, et al. "Real-time road slope estimation based on adaptive extended Kalman filter algorithm with in-vehicle data." Control and Decision Conference IEEE, pp. 6889-6894, 2017.

[9] Grip, Håvard Fjær. "Topics in State and Parameter Estimation for Nonlinear and Uncertain Systems." Department of Engineering Cybernetics, 2010.

[10] Liu G, Zhang Q, Xiong J, et al. "An Investigation of Calculation Method of Wheel Angular Acceleration in Anti-lock Braking System." IEEE International Conference on Information and Automation, pp. 840-843, 2008

[11] Z Yu, X Xia, L Xiong, T Qu. "Vehicle Longitudinal Velocity Nonlinear Adaptive Estimation of Distributed Drive Electric Vehicle." Journal of Tongji University 44.5, pp. 779-786, 2016.

[12] W Chu, Y Luo, et al. "Vehicle mass and road slope estimates for electric vehicles." Journal of Tsinghua University, pp.724-728, 2014.

[13] Jin, Chi, et al. "Path Following Control for Skid Steering Vehicles with Vehicle Speed Adaption." Sae Technical Papers, 2014.

[14] Xia X., et al. "Estimation of maximum road friction coefficient based on Lyapunov method." International Journal of Automotive Technology 17.6, pp. 991-1002, 2016.

[15] Kay, H. S., and H. K. Khalil. "Universal controllers with nonlinear integrators." American Control Conference, 2002. Proceedings of the IEEE, pp. 116-121,2002.